Consort 1 Sounding Rocket Flight

Francis C. Wessling*
University of Alabama in Huntsville, Huntsville, Alabama
and
George W. Maybee†
McDonnell Douglas Space Systems Company, Huntsville, Alabama

Materials processed in low gravity have been demonstrated to exhibit different characteristics than those processed on Earth under unit gravity. Density-driven sedimentation and convection are two factors that contribute significantly to these differences. To further investigate low-gravity effects, with the purpose of opening pathways to new technologies and commercial applications, a payload of six experiments has been developed for low-gravity flight using a sounding rocket. It is expected that this investigation will produce a wealth of new information for advancing both materials and life-sciences processing applications. This paper describes experiments and discusses rocket-payload integration and operations.

Introduction

THE Consortium for Materials Development in Space (CMDS) at the University of Alabama in Huntsville (UAH) has developed an experimental payload to investigate the effects of low gravity on materials processes. The payload contains six experiment systems, and hardware for experiment power, command and data distribution, and measurement of acceleration levels. A Starfire sounding rocket will carry the payload into a ballistic trajectory providing approximately 7 min of low gravity ($10^{-5}g$). The Starfire is a two-stage (TX664-4/Black Brant VC) solid-propellant launch vehicle. This mission, designated Consort 1, marks the first sounding rocket flight for low-gravity materials processing work by the United States since June 17, 1983.[1]

The objective of the Consort 1 mission is to obtain new data and samples from low-gravity experiments for analysis and comparison with ground-based control experiments and, in one case, with data from a space transportation system (STS) orbiter mission. Consort 1 will also establish the basis for follow-on payloads. The elimination of density-driven sedimentation and/or convection in low gravity is expected to play a significant role in all of the experiments. For reference, the payload consists of the systems tabulated in Table 1. The first six items in the table are the experiments; the last two items are for operation and support. Specific objectives and methods for individual experiments are described in the present paper.

Consort 1 is being carried out under the CMDS as part of an ongoing program to investigate materials processing in space and foster new technology for commercial applications. The experiments are all precursors to others that eventually will fly as orbital payloads on carriers in NASA's low-Earth-orbit infrastructure. A rocket flight that allows only minutes of low-gravity time is a logical first step for many experiments to be flown later on carriers of more limited availability. This approach also allows hardware and protocol to be verified and preliminary results to be obtained without the expense and long lead time typically associated with orbital research.

Payload volume is approximately $0.5m^3$: 0.44 m in diameter and 3.5 m in length. It is built up from smaller sections, each configured for independent checkout and servicing. Total payload mass, in flight-ready configuration, is 279 kg. To support experimental operations, the payload includes a nonpressurized compartment, a pressurized compartment, nonpropulsive vents, computer-controlled power and signal distribution, four battery packs, two accelerometers, and a telemetery output port. When integrated with the Starfire, payload telemetry lines are connected to the rocket telemetry system. This provides PCM/FM downlink transmission at 2259.5 MHz (S-band) for real-time data acquisition. During flight, experiments are activated, monitored, and deactivated by an onboard controller.

The payload was vibration tested to verify that it functions properly after experiencing a simulated Starfire launch environment. It has also undergone a series of operational test simulating the launch countdown and flight sequence of events. Prior to launch, the payload will be integrated with Starfire telemetry, guidance and recovery systems for spin balancing, additional vibration testing, and reverification of experiment operations.

The launch occurred March 29, 1989 from White Sands Missile Range, New Mexico. The expected flight profile is shown in Fig. 1. Low-gravity operations begin after second-stage separation and nullification of payload body rates to below = 0.6 deg/s roll, below = 0.1 deg/s pitch, and below = 0.1 deg/s yaw. This will occur approximately 72 s into the flight at an altitude of 106 km. After re-entry, at approximately 4.8-km altitude, the main parachute is deployed. Impact occurs 80 km downrange at a velocity of 9 m/s. Two helicopters will be deployed to recover the payload. Each will carry a three-man recovery team to the landing site where the payload will be separated into three sections and returned for postflight processing and experiment data retrieval.

Demixing of Aqueous Polymer Two-Phase Systems

When certain pairs of water-soluble polymers are mixed with water, a liquid–liquid two-phase system is formed. A common example of such an aqueous polymer two-phase system is that formed by solution of 5% polyethylene glycol (PEG) and 5% dextran in water. The resultant two-phase system is primarily aqueous (approximately 90%) and contains most of the PEG in the top phase and most of the dextran in the bottom phase; hence, the top phase is generally referred to as PEG rich and the bottom phase is generally referred to as dextran rich.

An apparatus (see Fig. 2) consisting of two rows of six glass cuvettes (1.5-m cubes) containing various immiscible liquids and stirring bars spun by small electric motors[2] mixes the liquids upon entering microgravity. The progress of demixing is then followed photographically. The apparatus has previously

Received Oct. 3, 1988; revision received March 7, 1989.

*Professor, Department of Mechanical Engineering. Member AIAA.
†Senior Technical Specialist. Senior Member AIAA.

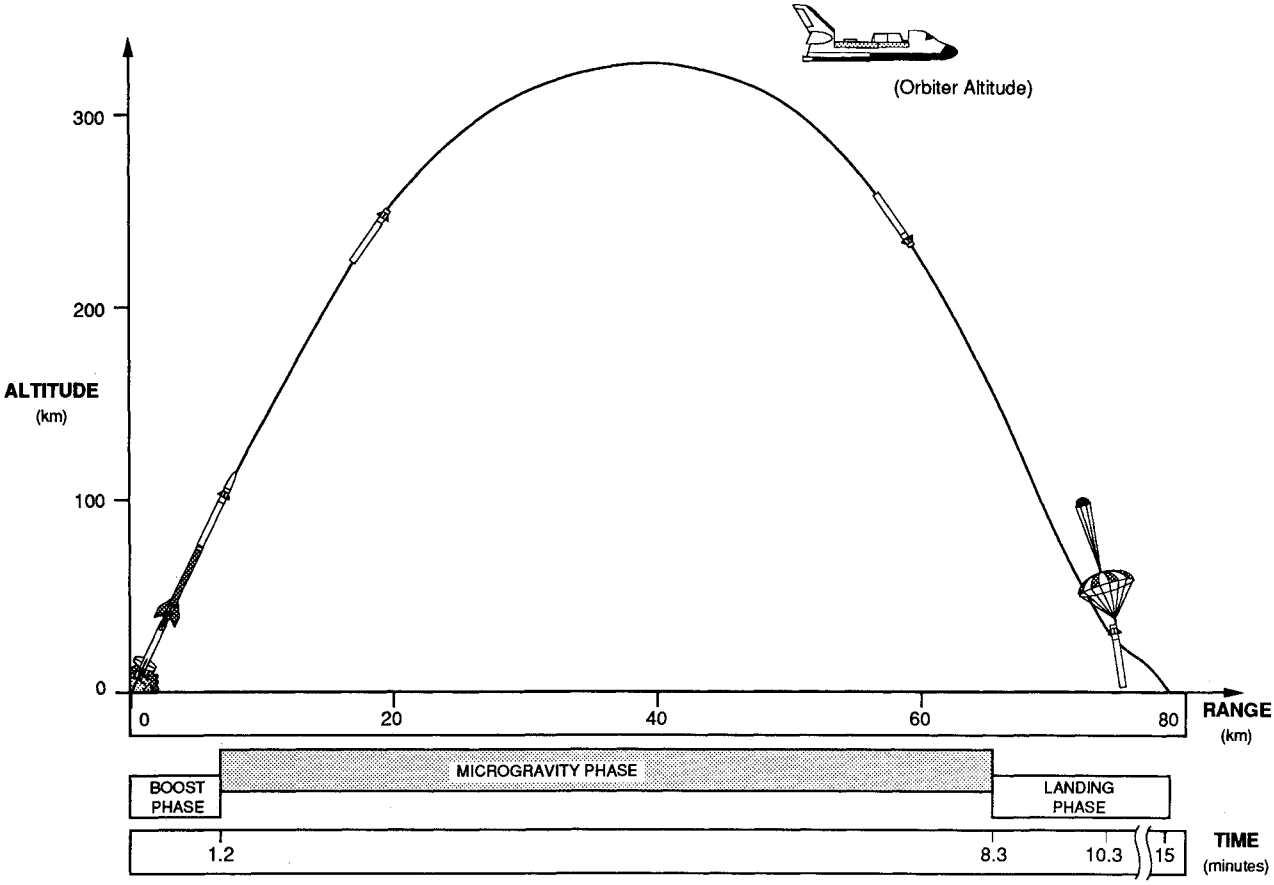

Fig. 1 Expected flight profile.

Table 1 Consort 1 payload experiments and investigators

Item	Principal investigator	Organization
Demixing of immiscible polymers mixer	J.M. Harris P. Concus	UAH, Dept. of Chemistry Univ. of Cal. Berkeley, Dept. of Mathematics
Electrodeposition cells	C. Riley G.W. Maybee	UAH, Dept. of Chemistry McDonnell Douglas Space Systems, Co.
Elastomer-modified epoxy resins heater	J.M. Harris F.C. Wessling J. Geibel	UAH, Dept. of Chemistry UAH, Dept. of Mechanical Engineering Consultant, Phillips Petroleum
Foam-formation device	S.P. McManus F.C. Wessling D. Weiker	UAH, Dept. of Chemistry UAH, Dept. of Mechanical Engineering Consultant, Hercules, Inc.
Materials dispersion apparatus	J. Cassanto	Instrumentation Technology Associates
Metal-sintering furnace	J.E. Smith	UAH, Chemical Engineering Program
Flight experiment computer	C.C. Rupp	Marshall Amateur Radio Club
Accelerometers	J. Bijvoet R. Newberry	CMDS CMDS

been flown on KC-135 low-gravity parabolic flights. Precursor experiments have flown on the Shuttle in simpler apparatus.

The interfacial tension in these two-phase systems is very low (approximately a thousand times less than that for a typical organic-water two-phase system) and they can be buffered with various salts. As a consequence, biological materials such as proteins and cells are quite stable in these systems. An important biological purification technique is based on this partitioning of materials between the two phases and the interface.[3,4] The systems also serve as transparent fluid models with which to study the fluid physics of demixing processes in polymer blends, polymer-gas foams, and metals. This knowledge is applicable to 1) providing a better understanding of the role of phase segregation and domain size and uniformity in determining the properties of polymer blends and polymer foams[5]; 2) modeling of demixing of immiscible metals[6]; and

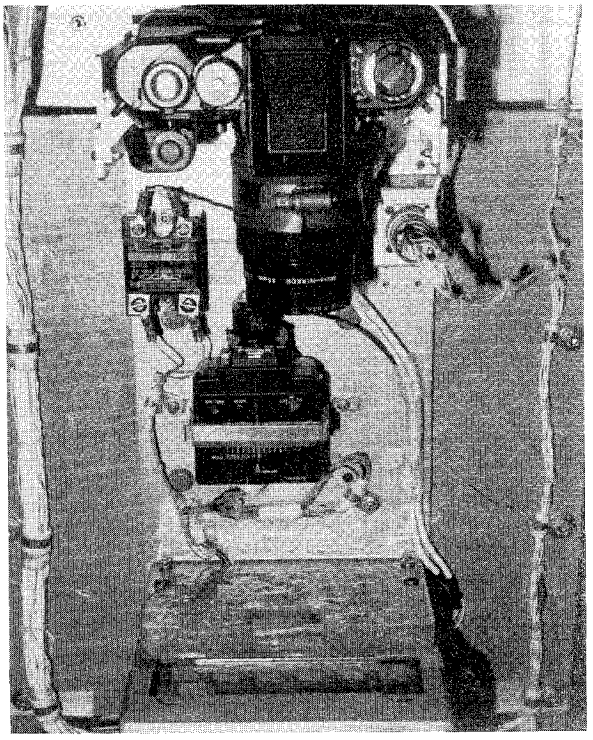

Fig. 2 Demixing of immiscible polymers mixer.

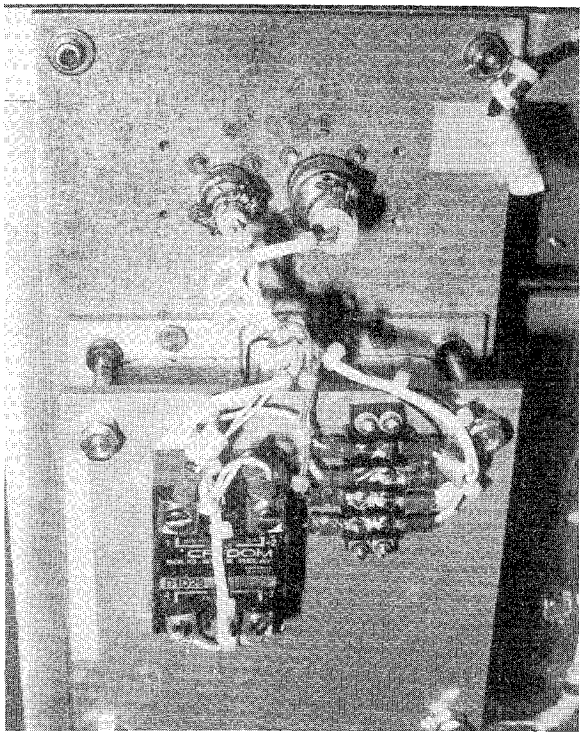

Fig. 3 Elastomer-modified epoxy resins heater.

3) purification of biological materials by partitioning between the two liquid phases formed in the aqueous polymer two-phase systems.

In Earth's gravity (unit g), demixing of aqueous polymer two-phase systems is quite rapid because of density-driven sedimentation; the dextran-rich layer is approximately 0.02 g/ml more dense than the PEG-rich layer. Until recently, it was not clear if a two-phase system would demix in low g. For example, all early experiments will oil and water[7] showed that this system did not demix after mixing in low g. In contrast, immiscible metals demix rapidly in low g.[8]

In a recent Shuttle experiment (STS 51G),[9,10] aqueous polymer two-phase systems were found to demix in low g, but at significantly lower rates (a matter of 5–10 min compared to 2–3 min, depending on the system) and more uniformly than in 1 g. The demixing process appears to proceed in two stages: first there is a coalescence process in which phase droplets grow until they approach the dimensions of the container at which point a second stage controlled by wall wetting sets in. Critical factors in controlling demixing rate were phase volume ratios and viscosity. Interfacial-tension effects were swamped by more powerful viscosity effects.

A key experiment now is to determine if the demixing *rate* and *location* of aqueous polymer two-phase systems can be controlled by changing the wall wetting[11] with polymer coatings on the container and by container shape.[12]

Wall wetting can be controlled with dextran coatings. The next step, and a critical part of the present experiment, is to determine if this control of wall wetting will 1) lead to control of location of the two phases in low g; i.e., will an inner sphere be dextran-rich when the PEG-rich phase wets the wall and shift to a PEG-rich inner sphere when the dextran-rich phase wets the wall; and 2) lead to control of demixing kinetics in low g. If the present hypothesis regarding a two-step demixing process is correct, then the demixing rate could be slowed by using a coating in which there is not a large preference for wall wetting by either phase (i.e., contact angle near 90 deg).

The second part of the present experiment will be to examine the effect of container shape on demixing location and rate. Previous work[12] has shown that certain critical contact angles can be defined for specific container shapes in which a liquid-liquid interface as obtained in unit g will be unstable in low g. The net result will be that one of the liquids will flow past the other to reach a new equilibrium position. Thus, the removal of gravity will result in preferentially wetting liquid flowing along the walls.

The goal of this second set of experiments will be to examine the effects of container shape and contact angle to determine if these parameters can be used to control the rate and location of the phases. There has been much work on the mathematics of equilibrium interface stability, but little is known about the dynamics of this process. The rocket experiments will provide information on this point. Container geometries will be chosen and contact angles controlled with wall coatings. Results of this experiment and other low g experiments are intended to be used for the design of equipment for separation of living cells. These living cells would be used as seeds for growth in culture media.

Elastomer-Modified Epoxy Resins

The results of the experiment may lead to a better understanding of the demixing process and may lead to better epoxy products. The addition of rubber to epoxy lowers the tensile strength approximately 28% and the modulus of elasticity approximately 21%, but increases the fracture energy by a factor of 20.[13] This experiment investigates the morphology and strength of elastomer-modified epoxy resins.

The most important chemical factors in the experiment are 1) the type of elastomers and their compatibility, 2) the effect of gel time on the morphology, and 3) the effect of curing past gelation on morphology. The mixtures are heated in a curing heater (see Fig. 3) that raises the temperature of the mixture from 20–200°C in approximately 2 min. The heater has a square cross section 114 mm on a side. The thickness of the heated space is variable. The heater requires approximately 325 W from a 28-V power supply. Consequently, this experiment has a dedicated battery.

The system selected for this experiment consists of three elastomer-modified epoxy resins. The elastomers are commercial products and are of the general class of materials called carboxy-terminated copolymers of butadiene and acrylonitrile (CTBN elastomers). These elastomers can be reacted with epoxy resins (typically a low molecular-weight epoxy resin) to yield an epoxy-capped elastomer. Because the

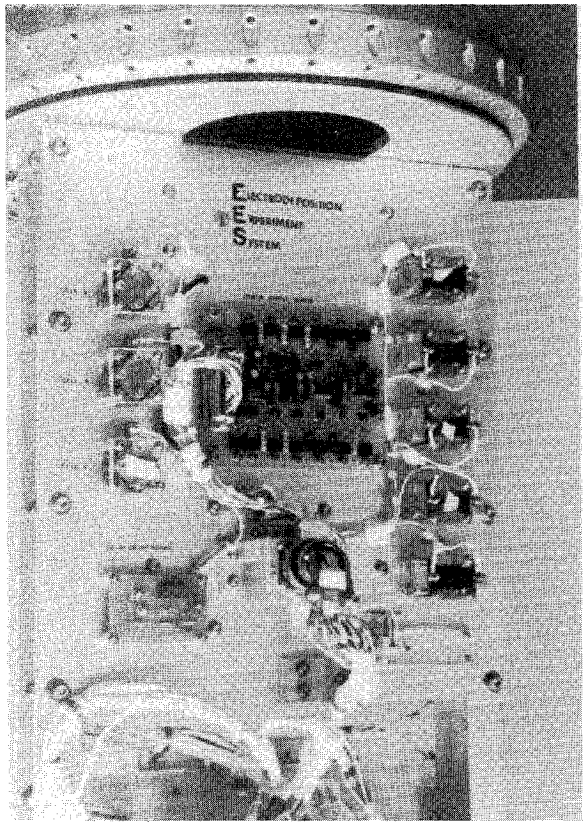

Fig. 4 Electrodeposition cells.

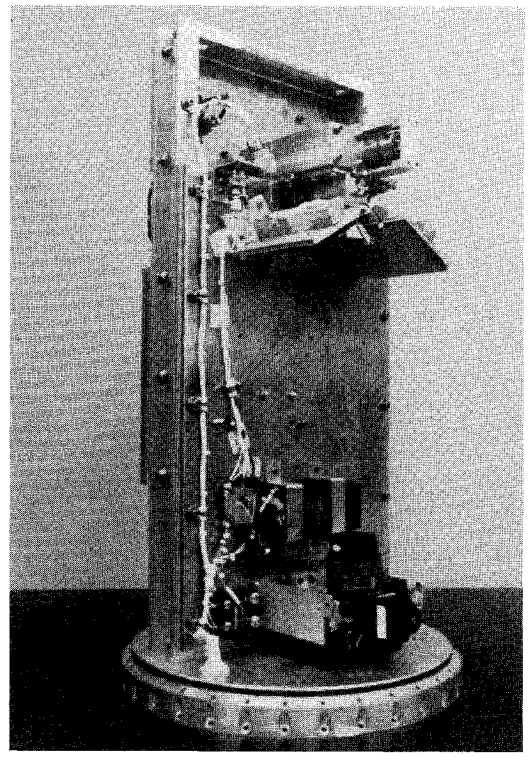

Fig. 5 Foam-formation device.

elastomer is capped by the epoxy resin, it can be cured just like a normal epoxy resin. However, because epoxy resins and the CTBN elastomers have different solubility parameters as the curing progresses, the driving forces for solubility decrease and the elastomer phase separates.[14] The curing process is slightly exothermic and the separated phases have different densities; thus, convective mixing may be influenced in the demixing process. The resultant deposition of rubber in epoxy will be determined by electron microscopy.[15] Previous experiments have shown that the resultant rubber globules are larger with increasing elastomer concentration. Rubber globules ranged in size from 0.02–1.2 um in diameter in previous work.

Electrodeposition

This experiment is part of a project concerned with the study of electrodeposition and electrocodepositon and applictions of these processes. As a result of these efforts, it is hoped to obtain a better understanding of 1) the role of convection and buoyancy in the mechanisms for formation of some electrodeposited surfaces, 2) the effect of electrodeposition rates coupled with low g upon deposited surface morphology, 3) concentration gradients in the vicinity of electrodepositing surfaces, 4) the effect of gravity upon the dispersion (coagulation) of neutral praticles that are codepositing, 5) the influence of (lack of) a moving medium upon codeposition, and 6) preparation of improved surface coatings and metal catalysts. For the Consort 1 flight, efforts will be directed toward the effect of electrodeposition rate in low g on the morphology of the deposited surfaces. In an attempt to "reproduce" the results of a German TEXUS experiment,[16] which reported formation of amorphous nickel, the TEXUS reported electrodeposition rate of 80 ma/cm^2 will be bracketed with a multiple cell package.

Three different sets of electrodeposition cells will be flown (see Fig. 4). One set will include five identically constructed cells. The electrodes are approximatley 2.0 cm^2 (1 cm $\times$ 2 cm) and are placed 3.4 cm apart. One cell, containing cobalt sulfate and boric acid, will operate at 1.0 V. Four cells, each containing nickel sulfamate, boric acid, and nickel chloride, will operate at different voltages (4.5, 6.0, 7.5, and 9.0 V) to provide a distribution of electrodeposition rates ranging from 33–120 mA/cm^2. A second set will include three cells with electrodes separated by 0.87 cm and with different surface areas (2.0, 1.0, and 0.5 cm^2). These cells will contain nickel sulfamate, boric acid, and nickel chloride and will operate at 2.5 V. The variable geometry and close spacing of the electrodes will yield three different and relatively high electrodeposition rates. Because of the high voltages, some gassing will occur during the electrodeposition period. Each of these cells will be provided with expansion chambers consisting of sealed collapsible tubing fitted into a machined groove in the side of the cell liquid cavity. The third set will consist of two cells that will undergo codeposition of a metal and neutral particles. In both cells, the electrodes are 3.4 cm apart and have surface areas of approximately 2.0 cm^2. One cell will contain nickel sulfamate with diamond dust and the other cobalt sulfate with chromium carbide. The cells will operate at 1.5 V. Prior to the application of cell voltage, the cell solutions are stirred to mix the neutral particles. This is accomplished by external magnets that are magnetically coupled with internal stirring bars. When the stirring motion has damped out, the codeposition process is initiated. These two cells are photographed in microgravity every 15 s.

The purpose of these experiments is to improve the understanding of the plating process, to determine if pure amorphous metals may be formed by electrodeposition, to determine any differences in catalytic activity between surfaces prepared in unit g and in low g, and to determine if there are improved characteristics of codeposited surfaces in low g.

Foam Formation in Low Gravity

Metal foam experiments were done on the Space Processing Applications Rocket (SPAR) series of rocket flights by using aluminum metal and argon gas on SPAR I and SPAR II[17,18] and copper oxide and carbon on SPAR X. The goal of this experiment, however, is to determine how the properties of polymer-gas foams are affected by preparation in low g. The basis for expecting a difference in properties between unit-g and low-g materials is that the gas bubbles in the low-g foam

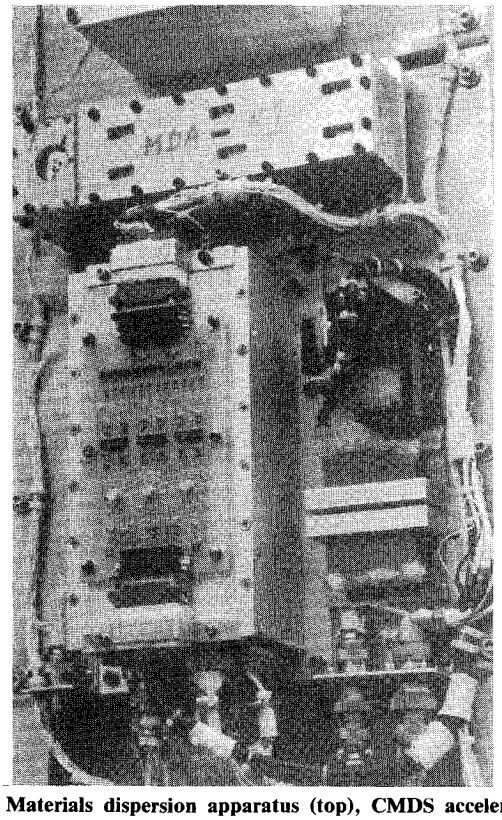

Fig. 6 Materials dispersion apparatus (top), CMDS accelerometer (right side), and controller (left side).

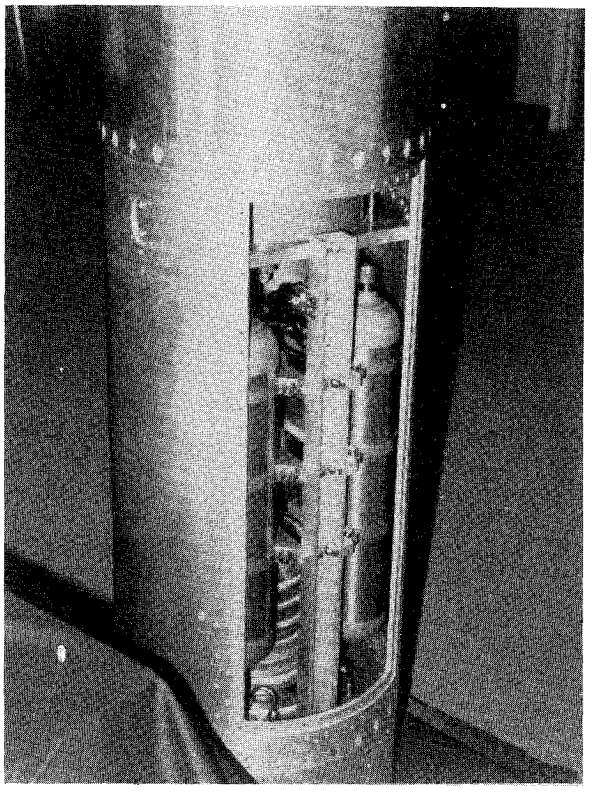

Fig. 7 Metal-sintering furnace.

should be more uniform. Foams made in Earth's gravity have nonuniform cell size partly because of the hydrostatic pressure of the foam. Also, previous liquid-liquid demixing experiments have shown that coalescence of immiscible fluids proceeds more slowly in the absence of gravity-driven sedimentation. Thus, bubble size can be expected to be smaller. Sedimentation and associated streaming will also lead to less uniform bubble distribution in the unit-g materials. In view of the importance of foams as construction materials, it is therefore of interest to determine if foams prepared in low g will have significantly different properties. This will lead to a better understanding of the foaming process.

The preparation of the foam begins with the activation of a gas-driven piston that forces isocyanate into a chamber filled with a mixture of polyol, catalyst, surfactant, and Fluorocarbon. The resultant mixture is stirred mechanically for 20 s. A second piston then drives the well-mixed liquids out of the mixing chamber through a funnel diffuser (see Fig. 5). Freon begins to come out of solution at the cream time, which occurs 28–37 s after mixing. Within 10 s of the cream time the material begins to expand. A 10–20 fold volume increase is achieved 180–200 s after the initial mixing. The foam reaches its final state after 120–180 s of additional cure. A successful experiment depends on each stage of the process (total of 300–360 s) occurring under a low-gravity environment. At this time, the foam is sufficiently hardened for survival through the landing. A foam volume of approximately 1800 cm^3 is expected. Photographs will be taken to record the cream and expansion process. The resultant foam will be further analyzed for thermal conductivity, mechanical strength, and cell size and distribution.

Materials Dispersion

The materials dispersion apparatus (MDA) (see Fig. 6) is a semiautomated, compact device that has the capability of mixing up to 100–200 samples in the 100–500 ml range for virtually any two fluids in space. In a typical experiment, different solutes are brought together across a quiescent liquid–liquid interface. The device occupies a volume of less than 0.11 m^3 and weighs less than 2.3 kg. The objective is to test the operation of the MDA in a microgravity environment for 6 min and allow samples to be mixed for multiple experiments.

Two blocks of inert material, each with an equal number of sample "cavities" in the upper and lower half, are held firmly together under pressure in a housing. The top block contains various samples of fluid A, such as a protein solution, while the bottom block contains samples of fluid B, such as a salt or other precipitating solution. The sample cavities are misaligned at the start of the experiment (prior to launch) thus separating the fluid samples to be mixed. After launch, when microgravity is attained, the blocks are moved into register with a motor and cam mechanism. When the sample cavities are aligned, their contents can mix. Upon signal, the blocks progress to an out-of-register position shortly before the end of microgravity.

Although the MDA was developed for mass production of protein crystals, some MDA units have been modified for fluid-science experiments such that an option is available to mix a third fluid during either the microgravity environment or prior to the reentry phase of the mission. The following fluid-science and biology experiments will be conducted using an MDA on the rocket flight: immiscible polymer phase separation, electrophoretic motion, turbulent mixing, solutal flow, cell fixation, protein crystal stability, solidification of organic metal models, protozoa growth, nucleation of crystals, diffusion coefficients, polymer thin-film membranes, and bone-marrow studies.

Metal Sintering

This experiment will examine the influences that low gravity has on reactive liquid-phase sintering of intermetallic alloys in a solid-phase matrix of nonmelting metal. Particular emphasis is being placed on those powered metal compacts which produce liquid alloys on sintering. For this class of materials, heating to a two-phase region causes the constituent components to react, forming an alloy liquid that must wet the solid

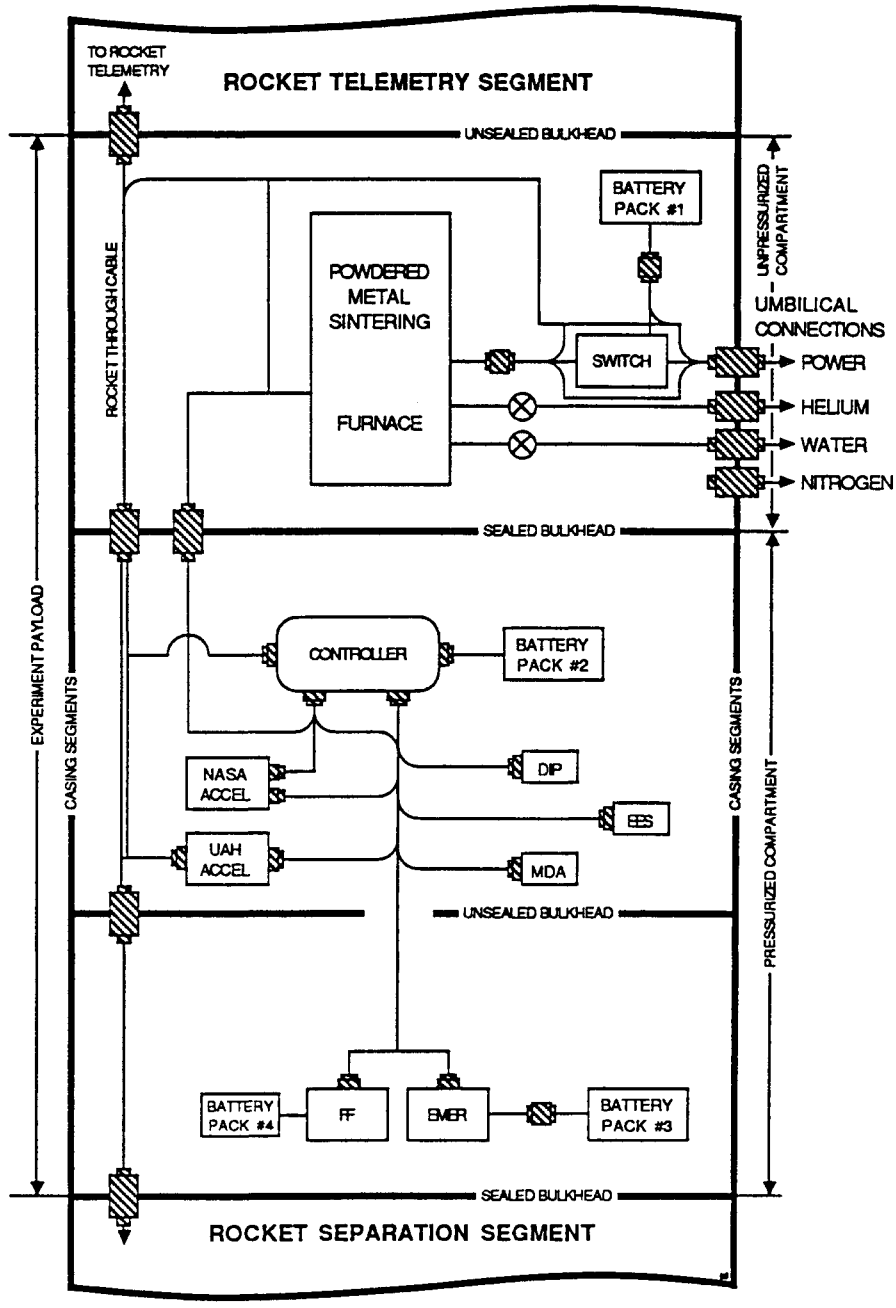

Fig. 8 Payload electrical schematic.

phase. Densification is initially driven by the free-energy effects that cause rapid rearrangement. Further densification occurs by evaporation and condensation, surface diffusion, bulk flow, and volume diffusion.

In unit gravity, sedimentation causes stratification within the sample that results in a nonuniform coarsening of microstructure. Sintering in a reduced-gravity environment should produce a smaller grain size, a more uniform microstructure possibly with less voids or defects, and improved mechanical properties.

The rocket furnace (see Fig. 7) is preheated on the launch pad to 1050°C. After launch, during the first part of the low-gravity period, the temperature is increased to 1040°C. A slow flow rate of helium (5 cm^3/s) is used to purge the system of oxygen during furnace operation. The furnace heating element is turned off and the helium flow rate is increased in order to cool the samples when the low-gravity period is almost over.

The furnace heating elements are insulated with solid zirconia. This is surrounded by a layer of silica-based fibrous batt insulation. The exterior of the furnace has a water jacket for cooling. The water is supplied from an 8-l bladder-pressured tank with an initial air pressure of 6 atm. The water flow continues until the rocket is recovered after landing or until the water supply is depleted. Both the helium and the water exit the rocket skin through nonpropulsive vents made from tubing tees, which are oriented at right angles to the longitudinal axis of the rocket.

Potential uses for liquid-phase sintered products include bearings, magnetic materials, electrical brushes and contact points, cutting tools, irregular-shaped mechanical parts for high-stress environments, and possibly new and improved catalysts for chemical production. Cutting tools for severe applications at the high linear cutting speeds used in modern manufacturing are of particular interest.

Accelerometers

The rocket will fly two accelerometers: one provided by the NASA Marshall Space Flight Center and one provided by the CMDS. The NASA accelerometer was designed for use on the space transportation system (STS). An earlier version was used in the materials experiment assembly in the orbiter bay of STS 7[19] and is similar to that flown on early SPAR rocket

flights.[20] The CMDS accelerometer is a newly developed system (see Fig. 6). The function of the accelerometer package is to measure low-g accelerations during the coasting part of the flight along three orthogonal axes.

The two accelerometer systems are installed at different locations to be used not only for the puposes of best estimation of the gravity field at different experiment locations but also for purposes of obtaining redundancy and gaining experience. Each accelerometer generates output signals proportional to the momentary acceleration level. These signals are sent to the ground in real time by telemetry and to the onboard experiment controller. The data is recorded onboard and on the ground for later analysis.

The NASA accelerometer is a hinged pendulum, fluid-damped, electrically restrained type. It uses an air core differential pickoff. The torquer used to restrain the pendulum is of a dc permanent magnet type. The full range output is $0.031g$ in each axis. Theoretical resolution of the output is 1.1×10^{-7} g/bit change/s. A sample output recording from a previous rocket flight shows a ripple of about 2×10^{-5} g and large spikes. The pulse rate of the accelerometers themselves is 2400 Hz. However, the acceleration data are integrated by the internal data-conditioning circuitry to fit a 1-Hz data rate because of its original application. The low-g measurement module uses three accelerometers mounted in an orthogonal triad on a temperature-stabilized mounting cube which offers better accelerometer stability. The cube is thermally isolated from the package to minimize power required by a proportional controller which maintains the temprature at 50–2°C. A full description of the NASA accelerometer is given in NASA Technical Memorandum TM-78211.[21]

The CMDS accelerometer is a linear servo instrument with a nonwearing elastic suspension. The full range of output of the CMDS accelerometer is $30g$ with a theoretical resolution of 1×10^{-6} g with a frequency response from 0–300 Hz. The accelerometer produces a current output that is directly proportional to the acceleration input. The accelerometer has an analog torque-balanced sensor with a fused quartz flexure, a permanent magnet torquer, a capacitive pickoff system, and self-contained servo electronics. The detector is made from amorphous quartz, is nearly perfectly elastic in the detector plane and nonelastic in all other planes[22]; and it is gas damped. Modeling data allows external temperature correction of the data. A temperature sensor is incorporated in the instrument.

The data from both accelerometers will be used to determine the acceleration levels and acceleration vectors at the locations of the experiments.

Experiment Controller

Developed initially for use in a get-away-special (GAS) cannister,[23] the experiment controller[24] (see Fig. 6) uses a low-power, high-performance single-board computer designed for control processing and data-logging applications. The software is capable of executing user software upon power-up using either machine code or Tiny Basic© user programs. The computer has one serial input/output port that is user programmable from 50–9600 baud has 32 channels of analog input two 8-bit programmable parallel ports plus one 5-bit port a central processing unit with a clock speed of 4 MHz and 32 kbytes of EPROM memory and 32 kbytes of RAM. It operates on 8–35 V dc power at 55 mA. Its dimensions are $255\times172\times83$ mm and has less than 2.4 kg mass.

The computer controls all of the onboard experiments with relays that power-up the various components. For example, the computer sends signals to charge camera strobe lights, take photographs, energize motors, and supply power to the furnace. The computer monitors the output from the NASA accelerometer along with other experiment data. The computer receives a signal when the rocket lifts off. The experiments will be started after a given elapsed time.

The telemetry output is driven by a universal asynchronous receiver transmitter (UART) operating at a bit rate of 1200 bits/s. All data acquired by the data system from the experiments are sent to the telemetry channel in real time. Data are also stored in nonvolatile memory for recovery after flight. A ground terminal consisting of a portable computer decodes the telemetry data and displays the data on a screen.

The rocket carries four battery packs which supply power to the experiments. Camera flash units carry their own dry cells. One battery pack supplies the furnace power, one supplies the elastomer-modified epoxy resins (EMER) heater, one supplies power to the stirring motor on the foam formation apparatus, and the other supplies the controller and all other experiment power.

A layout of the electrical interconnections for the payload can be seen in Fig. 8.

Payload Integration and Operations

The experiments are packaged in two compartments (see Fig. 9). The upper compartment is unpressurized and contains the powdered-metal sintering furnance, four helium gas cylinders, a water tank, associated plumbing and valves, a battery pack, and furnace electronics. This compartment is also equipped with nonpropulsive vents that are connected to the sintering furnace for helium and water-vapor discharge during furnace operations. The lower compartment is sealed, by means of o-rings and pressure bulkheads, to maintain 1 atm when in a vacuum. With the exception of the sintering-furnace system, all of the payload experiments and support systems are contained in this compartment because they require 1 atm for proper operation. It consists of two sections connected by a load-bearing bulkhead. The upper section houses the two accelerometers, a battery pack, the flight computer, and apparatus for the materials dispersion, demixing of immiscible polymers, and electrodeposition experiments. The lower section contains the apparatus for the elastomer-modified epoxy resin and foam – formation experiments.

The arrangement of hardware within the two payload compartments provides for centralization of the flight computer, which controls power distribution and command/data transmission. Hardware is also located to allow easy access while providing a balanced distribution of mass.

Both the pressurized and unpressurized compartments use the same means to mount the experiment hardware. Two longerons (C-channels) extend on opposite sides of the rocket longitudinal axis. Experiment hardware is mounted on plates attached to these longerons. One end of the longeron attaches to the bulkhead immediately above it and the other end to the bulkhead immediately below it. This allows each section to be assembled completely before the rocket casing is installed. It also allows experiment sections to be refurbished without modifying the rocket casing, which serves as a structural element.

Primary interfacing hardware within the payload includes longerons, bulkheads, mounting plates, power and signal cables, pressure seals, and fluid lines. The interfaces between the experimental payload and the sounding rocket systems include an unsealed bulkhead at the top, a sealed bulkhead at the bottom, and a cable that runs from top to bottom for transmission of control and data telemetry signals. A ground umbilical interface is provided in the upper payload compartment. This interface connects the experimental payload with ground power, water, helium, and nitrogen. All of these resources are required to operate the sintering furnace prior to liftoff. Ground power is also used for the flight computer and accelerometers during prelaunch operations. Twenty seconds before launch, the payload is switched to internal power, water, and helium. The ground support interface also links the payload with a ground control station for remote activation/deactivation commands. Remote ground control functions include ON/OFF of the flight computer, verification of computer activation, and ON/OFF switching for the sintering furnace.

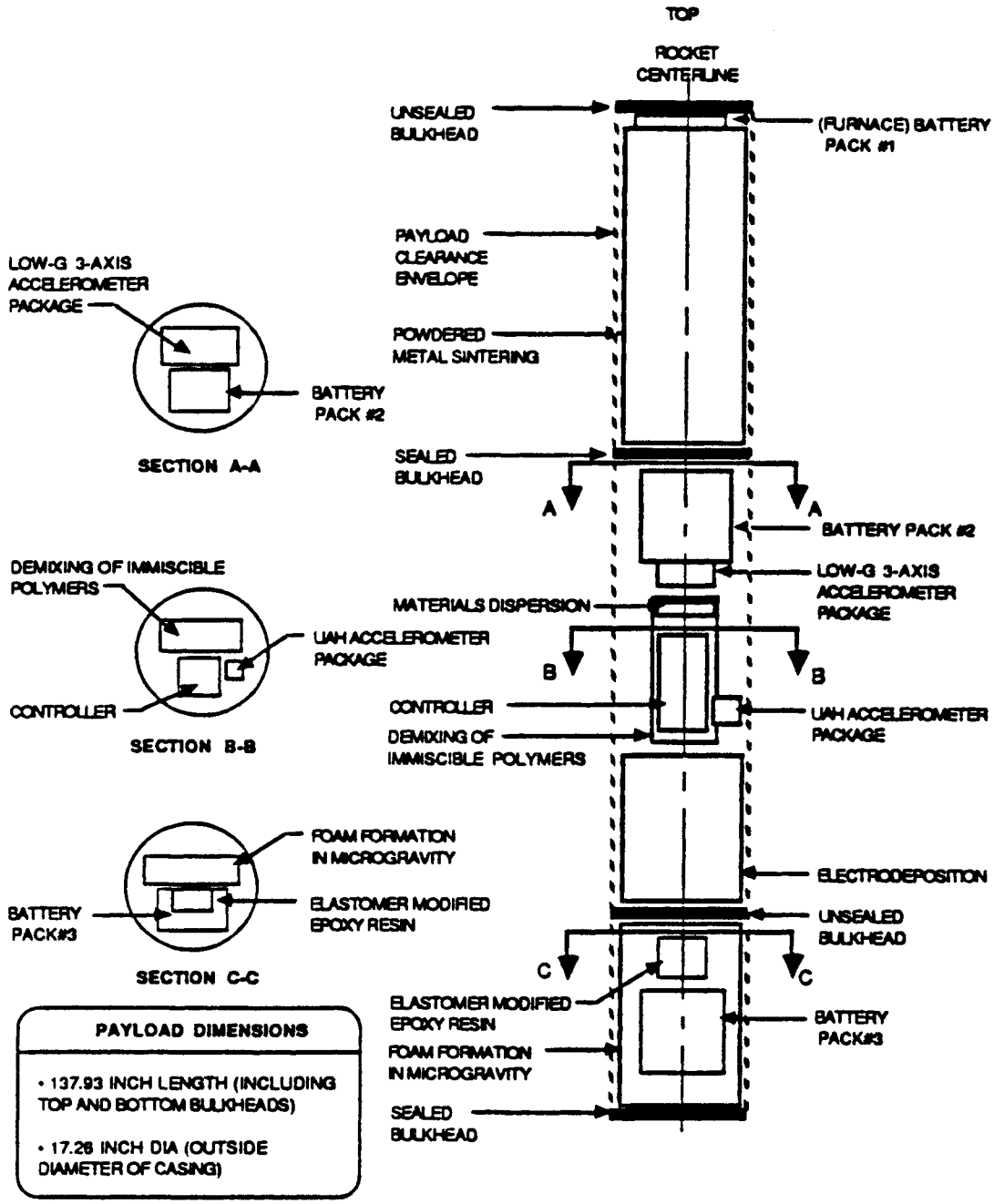

Fig. 9 Payload layout.

The payload has been designed for compatibility with the Starfire launch environment. A number of tests on individual and integrated systems have been performed to qualify the design and verify operations. Payload testing includes fluid line and pressurized compartment leak testing, vibration testing, and mission-sequence testing. The mission-sequence test exercises the complete mission operations timeline via the flight computer program. The vibration tests simulated the expected sounding rocket flight environment. Experiment systems have been vibration tested as individual packages and as part of the integrated payload configuration. Malfunctions that occurred during these tests were resolved by appropriate hardware modifications and the affected systems were verified by retest.

Summary and Conclusions

The 7 min of microgravity on the sounding rocket provides time for each of the experiments to gain needed microgravity information. The demixing of immiscible polymers experiment will be able to photograph the initial stages of demixing, and may be able to see some systems completely separated after their mixing in low gravity. In addition, the effect of container shape and liquid contact angle on demixing can be photographed. Ultimately, this information will be used for biological cell separation. The elastomer-modified epoxy resins experiment will yield samples processed in low gravity that are adequate for determining the morphology of these resins, as well as provide specimens for tensile testing. New forms of epoxy may ultimately emerge. The electrodeposition experiment will be able to obtain samples of nickel deposited over a range of current densities and also to obtain codeposited particles and metals for later analysis. These results may yield new forms of catalysts. A sample of polyurethane foam will be produced in low gravity. This sample will be analyzed for cell morphology and also for thermal conductivity and compressive strength. The foaming process will be photographed during microgravity to assist in understanding the formation process. A better understanding of the foam-

formation process should result. The materials dispersion apparatus will allow several researchers the opportunity to study a variety of phenomena including bone-marrow studies, organic cell growth, and diffusion phenomena. The small test chambers allow many researchers to perform experiments in a small volume. The metal-sintering furnace will be tested during flight and also will produce samples of a variety of powdered-metal combinations for later analysis. The output of the NASA accelerometer, which is flight proven, will be used to check the output of the CMDS accelerometer, which is newly developed. The NASA accelerometer delivers data each second in time, while the CMDS accelerometer data is telemetered as analog information. Successful operation of the CMDS accelerometer will lead to its use on later flights, not only on rockets but also on other low-gravity carriers. Thus, a variety of experiments will be performed with potential for future commercial applications.

Acknowledgments

This work is supported in part by the NASA Office of Commercial Programs under Grant NAGW-812. Payload trajectory and flight-sequence data were provided by Space Services, Inc. of America, the launch services contractor for the Starfire sounding rocket. Special thanks are due to the Marshall Amateur Radio Club and Mr. Charles C. Rupp for development of the experiment controller.

References

[1]Poorman, R., "SPAR X Final Report," Marshall Space Flight Center, NASA TM-86548, July 1986.

[2]Wessling, F., "Phase Partitioning, Crystal Growth, Electrodeposition, Cosmic Ray Experiments in Microgravity," NASA CP-2438, pp. Oct. 1986, 15-22.

[3]Karr, L. J., Shafer, S. G., Harris, J. M, Van Alstine, J. M., and Snyder, R. S., "Immunoaffinity Partition of Cells in Aqueous Polymer Two-Phase Systems," *Journal of Chromatography*, Vol. 354, May 1986, pp. 269-282.

[4]Harris, J. M. and Yalpani, M., *Polymer-Ligands Used in Partitioning in Aqueous Two-Phase Systems*, edited by H. Walter, D. E. Brooks, and D. Fisher, Academic, New York, 1985, Chap. 12.

[5]Brooks, E., Bamberger, S. B., Harris, J. M. and Van Alstine, J. M., "Rationale for Two-Phase Polymer System Microgravity Separation Experiments," European Space Agency, Paris, Vol. SP-222, Dec. 1984, pp. 315-318.

[6]Bamberger, S. B., Van Alstine, J. M., Baird, J. M., Harris, J. M., and Brooks, D. E., "Demixing of Aqueous Polymer Two-Phase Systems in the Absence of Gravity," *Separation Science Technology*, Vol. 23, Jan.-March 1988, pp. 17-34.

[7]Lacy, L. L., and Otto, G. H., AIAA Paper 74-1242, Oct. 1974.

[8]Feuerbacher, B., Hamacher, H., and Naumann, R. J., (eds.), *D. Beysens in Materials Science in Space*, Springer-Verlag, New York, 1986, pp. 191-224.

[9]Van Alstine, J. M., Harris, J. M., Synder, R. S., Curreri, P. A., Bambergr, S., and Brooks, D. E., "Separation of Aqueous Two-Phase Polymer Systems in Microgravity," European Space Agency, Paris, Vol. SP-222, Dec. 1984, pp. 309-313.

[10]Brooks, D. E., Bamberger, S. B., Harris, J. M., Van Alstine, J. M., and Synder, R. S., "Demixing Kinetics of Phase-Separated Polymer Solutions in Microgravity," European Space Agency, Paris, Vol. SP-256, Feb. 1987, pp. 131-138.

[11]Harris, J. M., Brooks, D. E., Boyce, J. F., Snyder, R. S., and Van Alstine, J. M., "Hydrophilic Polymer Coatings for Control of Electro-osmosis and Wetting," *Dynamic Aspects of Polymer Surfaces*, edited by J. D. Andrade, Plenum, New York, 1988, Chap. 8.

[12]Concus, P., "Equilibrium Fluid Interfaces in the Absence of Gravity," *Proceedings Symposium on Microgravity Fluid Mechanics*, American Society of Mechanical Engineers, New York, 1986, pp. 37-38.

[13]Riew, C. K., Rowe, E. H., and Siebert, A. R., "Rubber Toughened Thermosets," *Toughness and Brittleness of Plastics*, edited by R. D. Deanin and A. M. Crugnola, American Chemical Society, Washington, DC, 1976, pp. 326-343.

[14]Romanchick, W. A. and Geibel, J. F. "Characterization of Cured Epoxy Powder Coatings by Solvent Absorption," *Polymeric Materials for Electronic Applications*, ACS Symposium Series 184, American Chemical Society, Washington, DC, 1982, pp. 210.

[15]Romanchick, W. A., Sohn, J. E., and Geibel, J. F., "Synthesis Morphology and Thermal Stability of Elastomer-Modified Epoxy Resins," *Epoxy Resin Chemistry II*, ACS Symposium Series 221, American Chemical Society, Washington, DC, 1983, pp. 95-97.

[16]Ehrhardt, J., "Dispersion Electrolysis Under Zero Gravity," Under the Rocket Programs Texus VII and Texus IX, Nov. 1983 and Nov. 1984.

[17]Reeves, F. and Chassay, R., "SPAR II Final Report," Marshall Space Flight Center, NASA TM-X3458, Dec. 1976.

[18]Reeves, F. and Chassay, R., "SPAR II Final Report," Marshall Space Flight Center, NASA TM-78125, Nov. 1977.

[19]Harris, E. G., "Materials Experiment Assembly (MEA) Acceleration Summary," STS-7, Marshall Space Flight Center, JA62-004, July 1984.

[20]Toth, S. and Frayman, M., "Measurement of Acceleration Forces Experienced by Space Processing Applications," Goddard Space Flight Center Contract NAS5-23438, Mod 23, ORI Inc. TR-1308, March 1978.

[21]Amalavage, A. J., Fikes, E. H., and Berry, E. H. "Description of the Three Axis Low-*g* Accelerometer Package," Marshall Space Flight Center, NASA TM-78211, Nov. 1978.

[22]Peters, R. B. and Foote, S. A., "Computer Automated Testing of High-Performance/Price Ratio Instruments," *Instruments in the Aerospace Industry*, Vol. 29, *Advances in Test Measurement*, Vol. 20, Instrument Society of America, Research Triangle Park, NC, 1983, pp. 541-552.

[23]Stluka, E. F., "STS 61C Columbia Flight, Final Report," NASA CP-2438, Oct. 1986, pp. 87-93.

[24]Rupp, C. C., "Marshall Amateur Radio Club Experiment (MARCE) Postflight Data Analysis," NASA CP-2438, Oct. 1986, pp. 149-156.